

Diffusion-Aided Joint Source Channel Coding For High Realism Wireless Image Transmission

Mingyu Yang, Bowen Liu, Boyang Wang, Hun-Seok Kim
University of Michigan, Ann Arbor, MI, USA

Abstract—Deep learning-based joint source-channel coding (deep JSCC) has been demonstrated as an effective approach for wireless image transmission. Nevertheless, current research has concentrated on minimizing a standard distortion metric such as Mean Squared Error (MSE), which does not necessarily improve the perceptual quality. To address this issue, we propose DiffJSCC, a novel framework that leverages pre-trained text-to-image diffusion models to enhance the realism of images transmitted over the channel. The proposed DiffJSCC utilizes prior deep JSCC frameworks to deliver an initial reconstructed image at the receiver. Then, the spatial and textual features are extracted from the initial reconstruction, which, together with the channel state information (e.g., signal-to-noise ratio, SNR), are passed to a control module to fine-tune the pre-trained Stable Diffusion model. Extensive experiments on the Kodak dataset reveal that our method significantly surpasses both conventional methods and prior deep JSCC approaches on perceptual metrics such as LPIPS and FID scores, especially with poor channel conditions and limited bandwidth. Notably, DiffJSCC can achieve highly realistic reconstructions for 768×512 pixel Kodak images with only 3072 symbols (< 0.008 symbols per pixel) under 1dB SNR. Our code will be released in <https://github.com/mingyuang/DiffJSCC>.

Index Terms—deep joint source-channel coding, text-to-image diffusion models, Stable Diffusion, image captioning

I. INTRODUCTION

Traditional wireless image transmission typically involves a two-step process where an image is first compressed using image codecs (e.g., JPEG, BPG), and then protected with channel coding techniques (e.g., LDPC, Polar) over the wireless channel. However, since image codecs are not intrinsically designed to handle bit errors, the image reconstruction quality drops dramatically when channel coding fails to correct all errors - a phenomenon known as the “cliff effect”. To mitigate this issue, various joint source-channel coding (JSCC) methods have been proposed to improve the robustness of transmission errors [1], [2].

Recently, deep neural networks (DNNs) have demonstrated success in multiple domains such as computer vision [4], [5] and wireless communications [6]–[8], establishing them as a powerful tool to solve the JSCC problem. Bourtsoulatzé *et al.* [3] proposed the first deep learning-based JSCC (deep JSCC) framework for wireless image transmission where the image compression and error correction coding are jointly learned

This work was funded in part by NSF CAREER #1942806.

M. Yang, B. Liu, B. Wang, and H. Kim are with the Department of Electrical and Computer Engineering, University of Michigan, Ann Arbor, MI, 48109 USA e-mail: (mingyu@umich.edu; bowenliu@umich.edu; boyangwa@umich.edu; hunseok@umich.edu)

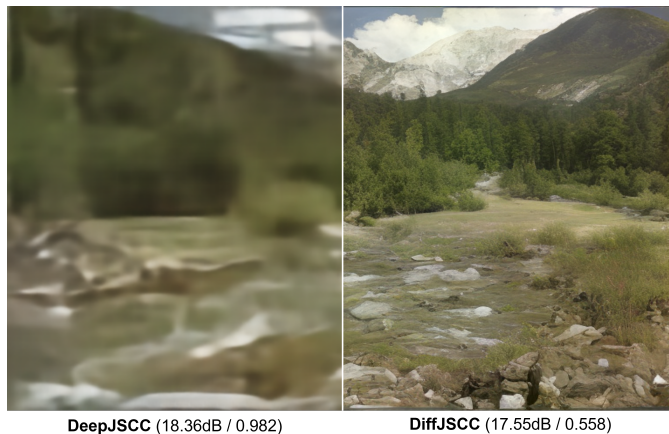


Fig. 1. Visual comparison between DeepJSCC [3] and the proposed DiffJSCC under an extremely low transmission rate ($R = 1/128$) and SNR ($\gamma = 1\text{dB}$). Each 768×512 image is transmitted with only 3072 complex symbols. The image quality is evaluated with PSNR/LPIPS.

through an autoencoder. This paradigm has demonstrated superior performance over traditional separate schemes under additive white Gaussian noise (AWGN) and Rayleigh flat fading channels. Following this study, the idea of deep JSCC was further extended with Transformer architectures [9], feedback channels [10], orthogonal frequency division multiplexing (OFDM) [11], and iterative refinement [12]. In the meantime, to enhance the flexibility of deep JSCC, a series of works were proposed to facilitate adaptability to various signal-to-noise ratios (SNR) [13] and transmission rates [14] for a single model. Despite their progress, the majority of existing works concentrate largely on minimizing image distortion through metrics such as Peak Signal-to-Noise Ratio (PSNR) and Structural Similarity Index Measure (SSIM). In scenarios with constrained bandwidth or poor channel conditions, the reconstructed image optimizing PSNR/SSIM tends to be blurry and often fails to capture detailed textures and global structures leading to degraded perceptual quality.

In tasks such as image compression and restoration, the issue of blurry artifacts is usually compensated through a generative model incorporating an adversarial loss [15], [16] or a diffusion model [17], [18]. Inspired by these works, Yang *et al.* [11] and Wang *et al.* [19] have combined deep JSCC with an adversarial loss based on PatchGAN [20]. Nevertheless, their performance is bottlenecked by the complexity of training a good Generative Adversarial Network (GAN) from scratch. Alternatively, Ecenaz *et al.* [21] proposed two frameworks to

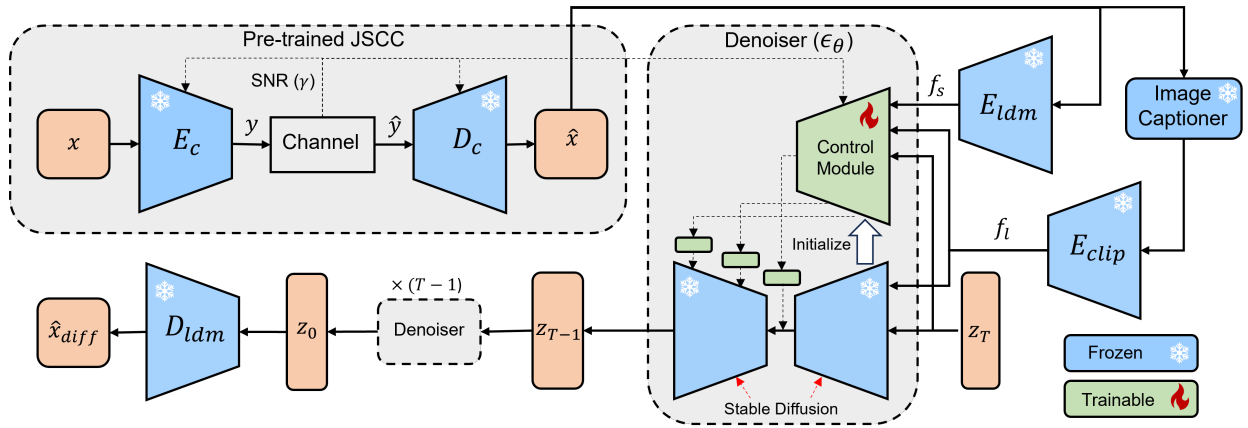


Fig. 2. The overall structure of the proposed DiffJSCC. A deep JSCC framework is first trained to obtain an initial reconstruction \hat{x} . Subsequently, \hat{x} undergoes spatial feature extraction through the Stable Diffusion’s VAE encoder and textual feature extraction through the pretrained image captioner and CLIP encoder. The generated spatial features f_s , textual features f_t and the channel SNR γ are fed to the control module as conditions. The control module is initialized with the Stable Diffusion checkpoints. The outputs of the control module pass through trainable 1×1 convolution layers and then add to the Stable Diffusion UNet decoder. This conditional denoising process is done T times to generate the final estimation \hat{x}_{diff} from the random noise z_T .

integrate deep JSCC with the pre-trained StyleGAN-v2 generator [22] and demonstrated higher perceptual quality for face image transmission. Recently, Yilmaz *et al.* [23] first combined deep JSCC with a pixel-space diffusion model following the DDNM [24] framework, achieving superior performance over [21] in both distortion and perceptual metrics. In their method, an image is separated into range-space and null-space. Only the contents in the range space are transmitted through deep JSCC, while the null-space details are purely generated by the diffusion model on the receiver side. However, this method falls short in realism when the range-space contents undergo severe distortion. Besides, the effectiveness of this method is also constrained by the domain gap between the diffusion model’s training data and the target evaluation datasets.

In this work, we introduce DiffJSCC, a framework designed to enhance the perceptual quality of JSCC reconstructions using the Stable Diffusion model [25], which is less computationally intensive compared to pixel-space diffusion models. DiffJSCC employs established deep JSCC frameworks for initial image reconstruction, and then applies the Stable Diffusion model to enhance the perceptual quality of the reconstructed image. Inspired by the method in [26], our scheme adopts a control module to fine-tune the Stable Diffusion model. Unlike the method in [23] where the initial JSCC reconstruction is directly involved in the denoising process, our DiffJSCC limits the role of the JSCC path as the initial reconstruction merely providing conditional features for the control module’s guidance. Therefore, the denoising process aligns with the original denoising diffusion probabilistic model (DDPM) and remains uninfluenced by the distortion of the JSCC output. Throughout the fine-tuning process, the Stable Diffusion model is kept unaltered to preserve its generative ability. Since the control module is fine-tuned specifically on the target dataset, the challenge of domain gaps in [23] is also eliminated. Our control module adopts the architecture of LAControlNet [26] and processes the spatial features extracted from the initial JSCC reconstruction. Besides, recognizing the

text-to-image nature of the Stable Diffusion model, we extract additional textual features from the initial reconstruction with a pre-trained image captioner and text encoder. The channel information, such as SNR, is also incorporated into the control module to provide additional guidance. Experiments on the Kodak dataset show that the proposed method achieves superior human-perceptual quality compared with conventional separate schemes and prior deep JSCC baselines, especially when the bandwidth is constrained in poor channel conditions.

II. PRELIMINARY

A. Deep Joint Source Channel Coding

Established deep JSCC frameworks consist of a pair of an encoder E_c and decoder D_c . The encoder E_c maps the input image $x \in \mathbb{R}^{C \times H \times W}$ into channel symbols $y = E_c(x) \in \mathbb{C}^K$ for wireless transmission, which are usually normalized to unit power. The wireless channel is modeled as a conditional distribution and the received symbol can be retrieved by sampling $\hat{y} \sim p(y|\varepsilon)$, where ε denotes the channel parameters. The received symbols are then passed through the decoder D_c to obtain the image reconstruction $\hat{x} = D_c(\hat{y}) \in \mathbb{R}^{C \times H \times W}$. The transmission rate R is quantified by channel per pixel (cpp), which is defined as:

$$R = K/HW \text{ cpp.} \quad (1)$$

With a distortion function $d(x_1, x_2)$, the encoder and decoder can be trained end-to-end via:

$$\mathcal{L}_{JSCC} = \mathbb{E}_{x, \hat{y}} [d(x, D_c(\hat{y}))]. \quad (2)$$

B. Latent Diffusion Models

DDPM, as introduced by Ho *et al.* [27], aims to approximate a data distribution by incrementally refining a sample from a standard Gaussian distribution towards the desired data through a series of denoising steps. To improve the efficiency and stability of the training process, Rombach *et al.* [25] introduced Stable Diffusion, where a variational autoencoder

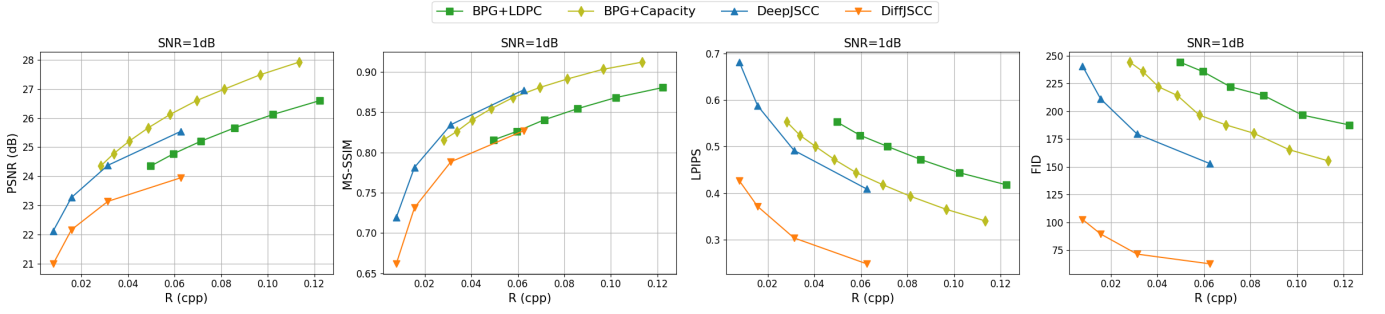


Fig. 3. Comparison between the proposed method and baselines at various transmission rates with 1dB SNR on the Kodak dataset.

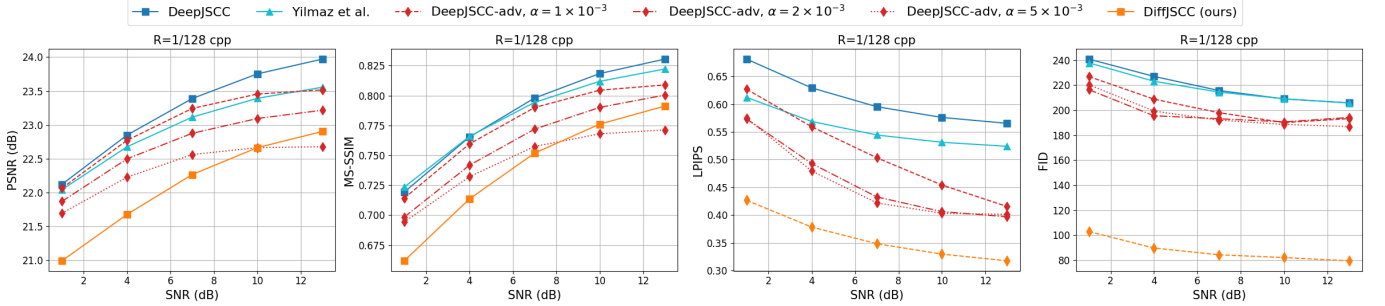


Fig. 4. Comparison between the proposed method and baselines at various SNRs with a transmission rate of 1/128 cpp on the Kodak dataset.

(VAE) is pre-trained to map images to low-dimensional latent space. The diffusion process is then performed in the latent space. In the forward diffusion process, a Gaussian noise with variance $\beta_t \in (0, 1)$ is added to the latent z_{t-1} at time step t . Summarizing the diffusion process from step 1 to t , the latent z_t can be expressed as:

$$z_t = \sqrt{\bar{\alpha}_t} z_0 + \sqrt{1 - \bar{\alpha}_t} \epsilon, \quad (3)$$

where $z_0 = E_{ldm}(x)$ is the original encoded latent, $\epsilon \sim \mathcal{N}(0, \mathbf{I})$, $\alpha_t = 1 - \beta_t$ and $\bar{\alpha}_t = \prod_{i=0}^t \alpha_i$.

The denoising process aims to find the previous state z_{t-1} using the posterior $p(z_{t-1}|z_t, z_0) = \mathcal{N}(z_{t-1}; \mu_t(z_t, z_0), \sigma_t^2 \mathbf{I})$, where the mean can be parametrized as:

$$\mu_t(z_t, z_0) = \frac{1}{\sqrt{\alpha_t}} \left(z_t - \epsilon \frac{1 - \alpha_t}{\sqrt{1 - \bar{\alpha}_t}} \right). \quad (4)$$

Then, to sample z_t , the task is essentially to predict the noise ϵ and this is handled by a network ϵ_θ . This prediction is often conditioned on a context variable c , which may include additional information such as text prompts. The network ϵ_θ can be trained with:

$$\mathcal{L}_{ldm} = \mathbb{E}_{z_0, c, t, \epsilon} \|\epsilon - \epsilon_\theta(\sqrt{\bar{\alpha}_t} z_0 + \sqrt{1 - \bar{\alpha}_t} \epsilon, c, t)\|_2^2. \quad (5)$$

III. METHODS

The overview of DiffJSCC is shown in Fig. 2. We first train a deep JSCC model in line with prior works and obtain the initial JSCC reconstruction \hat{x} (Section III-A). Then, we leverage the prior knowledge of the Stable Diffusion model and finetune a control module conditioned on the features extracted from \hat{x} and the channel information (Section III-B).

A. Channel Model and Deep JSCC

In this paper, we mainly consider the Additive White Gaussian Noise (AWGN) channel, where the received symbols \hat{y} are sampled through:

$$\hat{y} = y + w, \quad w \sim \mathcal{CN}(0, \sigma^2 \mathbf{I}_K), \quad (6)$$

where σ denotes the power of the channel noise. The channel SNR γ is computed as $\gamma = P/\sigma^2$ where P denotes the power of the transmitted signal. Note that the AWGN channel is fully differentiable and thus the entire deep JSCC model is end-to-end trainable.

We adopt the SNR-adaptive deep JSCC structure introduced in [14] where the channel SNR is assumed to be known by both the transmitter and receiver during transmission. Such information is explicitly integrated with the encoder and decoder, which leads to $y = E_c(x, \gamma)$ and $\hat{x} = D_c(\hat{y}, \gamma)$. The SNR information is fused with intermediate features via the Squeeze-Excitation structure [28]. Since we are not considering the problem of automatic rate control, the transmission rate is fixed for each model and the policy network is omitted. The transmission rate R is controlled by the number of output channels C_{out} and the downsampling factor D . We fix the downsampling factor to $D = 4$, and the transmission rate R can be controlled by $R = C_{out}/(2^4 \times 2^4 \times 2) = C_{out}/512$. To train the deep JSCC model, we adopt Mean Squared Error (MSE) as our distortion function following prior works. It is worth noting that our approach remains model-agnostic, providing flexibility to integrate more sophisticated deep JSCC structures if desired.

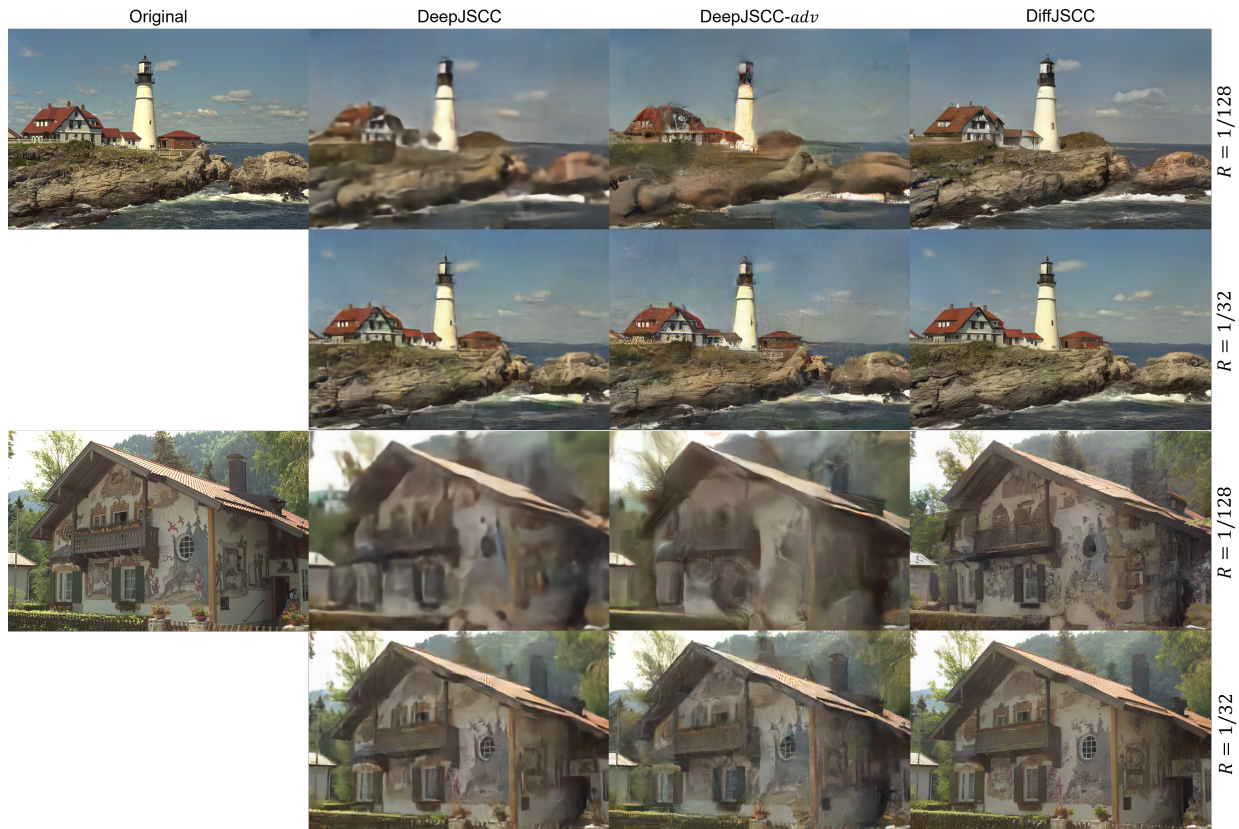


Fig. 5. Visual comparison between the proposed DiffBIR and baselines on the Kodak dataset (Zoom in for best view). All images are transmitted with $R = 1/32$ cpp or $R = 1/128$ cpp at 1dB SNR.

B. Leveraging the Generative Priors

Our denoiser network, denoted by ϵ_θ , follows a similar structure as LAControlNet [26] which contains the original denoiser UNet in Stable Diffusion and a control module. The denoiser UNet from the Stable Diffusion model contains an encoder, a middle block, and a decoder, and it is always kept fixed to maintain its intrinsic generative ability. The controller module mirrors the structure of the UNet’s encoder and middle block and inherits their parameters as initialization. For feature extraction, we pass the initial JSCC reconstruction \hat{x} through the pre-trained VAE encoder E_{ldm} of the Stable Diffusion Model to acquire the spatial feature f_s , which is then concatenated with the input noise z_t and passed to the control module. Besides, leveraging the text-to-image generation proficiency of the Stable Diffusion model, we further extract the textual information hidden in the initial JSCC reconstruction \hat{x} using a pre-trained image captioner BLIPv2 [29] to generate image captions followed by the pre-trained CLIP text encoder to extract the textual features f_t . Subsequently, f_t is treated as the text prompts and incorporated with the cross-attention blocks in both the control module and the original denoising UNet. In addition, we innovatively explore the usage of channel SNR as another guidance signal to the control module. We introduce another embedding module to map the channel SNR γ to embedding vectors that match the dimension of the time embeddings. Then, the SNR-related embedding is added to

the time embedding and conveyed to the controller module. The multi-level outputs of the control module (shown in the dotted arrows) are added to the original UNet decoder after passing through 1×1 convolutional layers. All the additional 1×1 convolutional layers are initialized with zeros. The entire denoiser network ϵ_θ can be trained as:

$$\mathcal{L}_{ldm} = \mathbb{E}_{z_0, t, \epsilon} \|\epsilon - \epsilon_\theta(\sqrt{\alpha_t}z_0 + \sqrt{1 - \alpha_t}\epsilon, f_s, f_t, \gamma, t)\|_2^2. \quad (7)$$

IV. EXPERIMENTS

A. Dataset and Training Details

We train DiffJSCC on a subset of the OpenImage dataset¹, which consists of 154k high-quality images. The deep JSCC model is trained on random image crops of size 256×256 pixels with a batch size of 32. We adopt the Adam optimizer with an initial learning rate of 10^{-3} . The training spans 100k iterations with a cosine decay schedule. The control module, which utilizes the Stable Diffusion 2.1-base as the generative prior, is fine-tuned on 512×512 resized images, employing a batch size of 16 for 25k iterations with a learning rate of 10^{-4} . Throughout the control module’s training phase, the deep JSCC model remains fixed. While training both the deep JSCC model and the control module, the SNR γ is uniformly sampled within the range of $[0, 14]$ dB. All the training processes are conducted using 2 NVIDIA A40 GPUs.

¹<https://storage.googleapis.com/openimages/web/index.html>

We test our model on the Kodak dataset, which contains 24 768×512 images. During inference, we use spaced DDPM sampling for 100 steps for the diffusion model.

B. Metrics

Our evaluation protocol incorporates widely recognized distortion metrics such as PSNR and MS-SSIM. To assess the perceptual quality of the reconstructions, we also employ Learned Perceptual Image Patch Similarity (LPIPS) and Fréchet Inception Distance (FID) scores [30]. To ensure robust evaluations, each image is transmitted 5 times. Given the limited number of images available for testing, the FID score is calculated using half-overlap 256×256 image patches.

C. Comparison with Baselines

In Fig. 3, we compare DiffJSCC with two conventional separate methods, alongside the baseline deep JSCC framework without any enhancements (designated as DeepJSCC). We test for multiple transmission rates while maintaining a constant SNR of 1dB. For the separate methods, we employ the Better Portable Graphics (BPG) codec² for image compression and the Low-Density Parity-Check (LDPC) codes specified in the IEEE 802.11n WiFi standard with a block length of 1944. At an SNR of 1dB, we utilize a coding rate of 2/3 for the LDPC and apply Binary Phase Shift Keying (BPSK) as the modulation technique. We explore a range of quantization levels (varying from 51 to 0) to span different transmission rates. Besides, we also use channel capacity as an upper bound of any channel coding schemes, which is computed via $C = \log_2(1 + \gamma)$. For deep JSCC schemes, we test for 4 transmission rates: $R = 1/128, 1/64, 1/32$, and $1/16$. As illustrated in Fig. 3, the deep JSCC scheme, even without enhancement, already outperforms the conventional separate schemes in most scenarios, correlating with the results reported in prior works. As the generative prior is employed, some performance degradation can be observed in conventional distortion metrics, evidenced by an approximate drop of 1.5dB in PSNR and 0.06 in MS-SSIM. Nevertheless, DiffJSCC provides a substantial improvement in LPIPS and the FID score, offering an approximate reduction of 0.26 and 140 in LPIPS and the FID score. The advantage of DiffJSCC becomes more significant when compared to conventional separate schemes, particularly in its capacity to provide highly realistic reconstructions at transmission rates unattainable by BPG+Capacity. Remarkably, the FID score of DiffJSCC at rate $R = 1/128 = 0.0078$ is lower than that of BPG paired with channel capacity at rate $R = 0.113$. These advantages demonstrate the effectiveness of DiffJSCC in generating high-realism JSCC image reconstructions.

Next, in Fig. 4, we compare DiffBIR with other generative JSCC baselines. We implement the DeepJSCC-adv algorithm proposed in [11] where α is used to control the weight of the adversarial loss. We explore multiple α values to balance distortion and realism. Besides, we also compared DiffJSCC

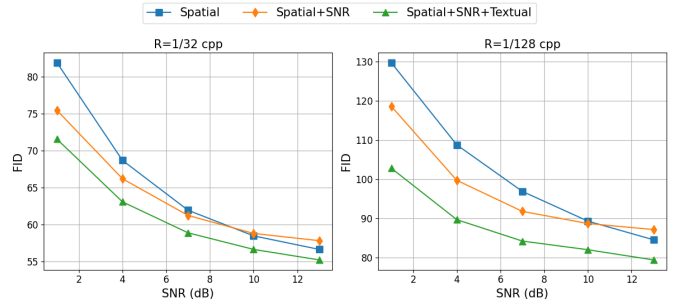


Fig. 6. Comparison of using different conditions to fine-tune the control module. The channel SNR is fixed to 1dB.

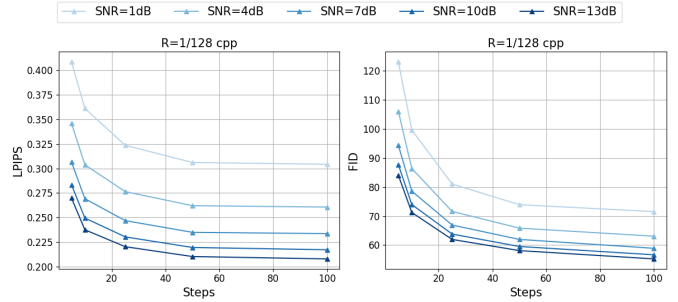


Fig. 7. Effect of DDPM sampling steps for various SNRs with $R = 1/128$.

with the method proposed in [23]. To ensure a fair comparison, we slightly modify [23] to accommodate it to the Stable Diffusion model. Specifically, in each denoising step, we initially decode the estimated original latent to the image space and conduct the original DDNM guidance. Then, we remap the output image back to the latent space to get the corrected latent. Similarly, we adopt the 2×2 average pooling as the degradation function. The experiments are conducted with $R = 1/128$ and across a span of SNRs $\gamma = 1, 4, 7, 10, 13$ dB. For all baselines, we adopt the same deep JSCC structure. As illustrated in Fig. 4, the baseline generative JSCC methods could somewhat reduce the LPIPS but fail to effectively reduce the FID score, which remains over 180. The proposed DiffJSCC, in contrast, manages to substantially reduce both LPIPS and the FID score. Note that the method [23] adopts the same Diffusion model as DiffJSCC in our experiment. Thus, the prominent improvement in perceptual quality illustrates the effectiveness of finetuning the Stable Diffusion model with the control module.

Furthermore, we provide visualizations in Fig. 5 to showcase the superior perceptual quality achieved by DiffJSCC. With $R = 1/128$, the DeepJSCC reconstruction is highly distorted and fails to recover crucial details. In comparison, DiffJSCC produces the best perceptual quality and successfully restores the key structures of the lighthouse and the house, despite minor deviations from the source image. When the transmission rate is increased to $1/32$, the DiffJSCC continues to outperform, and the generated contents are more aligned with the source image.

²<https://bellard.org/bpg/>

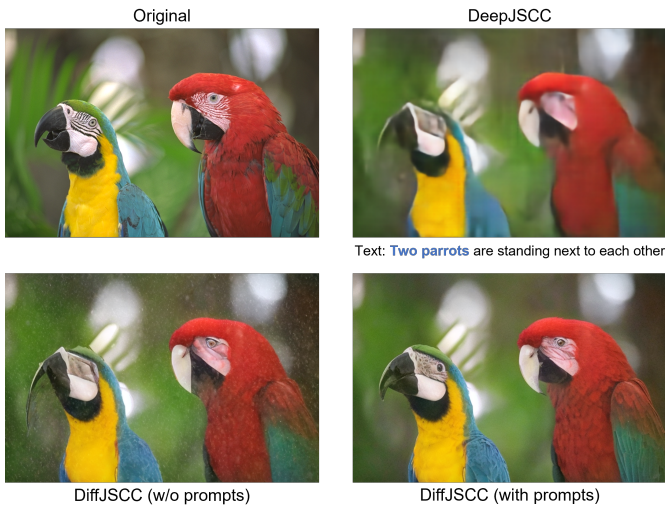


Fig. 8. Example of generated image captions and the effect of them for the final image reconstruction.

D. Ablation Studies

1) *The effect of different conditions:* In this section, we evaluate the impact of various conditional signals on the control module’s performance, as depicted in Fig. 6. It can be observed that relying solely on spatial features derived from the initial JSCC reconstruction yields suboptimal results. The integration of channel SNR as an auxiliary condition leads to a noticeable enhancement in FID scores, particularly at lower SNRs. This improvement shows that it is imperative to incorporate the channel state information into the denoising model to facilitate its adaptability across diverse distortion scenarios with different SNRs. Moreover, appending textual prompts to the control module further boosts the system performance, emphasizing the pivotal role of the textual context in the JSCC reconstruction problem. To better illustrate the impact of texts, we provide one representative example shown in Fig. 8. Despite the blurriness and distortion apparent in the initial JSCC reconstruction, the BLIPv2 model can extract coherent text prompts capturing the core semantic content of the image. In the absence of textual cues, our approach can still enhance the visual clarity but does not adequately restore the parrot on the left side of the image. However, with the incorporation of text prompts, there is a significant improvement in the fidelity of the left parrot’s reconstruction where finer details, such as the bird’s eyes, are successfully recovered.

2) *The effect of sampling steps:* We further examine the influence of varying the number of sampling steps in DDPM and the results are shown in Fig. 7. A progressive enhancement in both LPIPS and FID metrics can be observed as the number of sampling steps increases. Notably, the saturation point is reached around 100 steps, validating the decision of using 100 sampling steps in all of our experiments.

V. CONCLUSION

We propose DiffJSCC, an innovative deep JSCC framework that leverages the strong priors of the pre-trained Stable

Diffusion model to significantly enhance the perceptual quality of reconstructed images. DiffJSCC efficiently harnesses both spatial and textual features extracted from the primary JSCC reconstruction, merging them with channel state information. These combined multi-modal conditions are then fed to a control module to finetune the Stable Diffusion model. Through extensive experiments on the Kodak dataset, we demonstrate that DiffJSCC outperforms existing generative JSCC approaches considerably and delivers notably superior human-perceptual image quality, particularly in scenarios constrained by low transmission rates and unfavorable SNRs.

REFERENCES

- [1] V. Bozantzis and F. Ali, “Combined vector quantisation and index assignment with embedded redundancy for noisy channels,” *Electronics Letters*, vol. 36, no. 20, p. 1, 2000.
- [2] D. Goodman and T. Moulosley, “Using simulated annealing to design digital transmission codes for analogue sources,” *Electronics letters*, vol. 24, no. 10, pp. 617–619, 1988.
- [3] E. Boursoulatzé, D. B. Kurka, and D. Gündüz, “Deep joint source-channel coding for wireless image transmission,” *IEEE Transactions on Cognitive Communications and Networking*, vol. 5, no. 3, pp. 567–579, 2019.
- [4] S. Shoori, M. Yang, Z. Fan, and H.-S. Kim, “Efficient computation sharing for multi-task visual scene understanding,” in *Proceedings of the IEEE/CVF International Conference on Computer Vision*, 2023.
- [5] B. Wang, F. Yang, X. Yu, C. Zhang, and H. Zhao, “Apir: Anime production inspired real-world anime super-resolution,” *arXiv preprint arXiv:2403.01598*, 2024.
- [6] H. Ye, G. Y. Li, and B.-H. Juang, “Power of deep learning for channel estimation and signal detection in ofdm systems,” *IEEE Wireless Communications Letters*, vol. 7, no. 1, pp. 114–117, 2017.
- [7] M. Yang, L.-X. Chuo, K. Suri, L. Liu, H. Zheng, and H.-S. Kim, “ilps: Local positioning system with simultaneous localization and wireless communication,” in *IEEE INFOCOM 2019-IEEE Conference on Computer Communications*. IEEE, 2019, pp. 379–387.
- [8] Y.-S. Hsiao, M. Yang, and H.-S. Kim, “Super-resolution time-of-arrival estimation using neural networks,” in *2020 28th European Signal Processing Conference (EUSIPCO)*. IEEE, 2021, pp. 1692–1696.
- [9] K. Yang, S. Wang, J. Dai, K. Tan, K. Niu, and P. Zhang, “Witt: A wireless image transmission transformer for semantic communications,” in *ICASSP 2023-2023 IEEE International Conference on Acoustics, Speech and Signal Processing (ICASSP)*. IEEE, 2023, pp. 1–5.
- [10] D. B. Kurka and D. Gündüz, “Deepjssc-f: Deep joint source-channel coding of images with feedback,” *IEEE Journal on Selected Areas in Information Theory*, vol. 1, no. 1, pp. 178–193, 2020.
- [11] M. Yang, C. Bian, and H.-S. Kim, “Ofdm-guided deep joint source channel coding for wireless multipath fading channels,” *IEEE Transactions on Cognitive Communications and Networking*, vol. 8, no. 2, pp. 584–599, 2022.
- [12] C. Lee, X. Hu, and H.-S. Kim, “Deep joint source-channel coding with iterative source error correction,” in *International Conference on Artificial Intelligence and Statistics*. PMLR, 2023, pp. 3879–3902.
- [13] J. Xu, B. Ai, W. Chen, A. Yang, P. Sun, and M. Rodrigues, “Wireless image transmission using deep source channel coding with attention modules,” *IEEE Transactions on Circuits and Systems for Video Technology*, vol. 32, no. 4, pp. 2315–2328, 2021.
- [14] M. Yang and H.-S. Kim, “Deep joint source-channel coding for wireless image transmission with adaptive rate control,” in *ICASSP 2022-2022 IEEE International Conference on Acoustics, Speech and Signal Processing (ICASSP)*. IEEE, 2022, pp. 5193–5197.
- [15] E. Agustsson, M. Tschannen, F. Mentzer, R. Timofte, and L. V. Gool, “Generative adversarial networks for extreme learned image compression,” in *Proceedings of the IEEE/CVF International Conference on Computer Vision*, 2019, pp. 221–231.
- [16] F. Mentzer, G. D. Toderici, M. Tschannen, and E. Agustsson, “High-fidelity generative image compression,” *Advances in Neural Information Processing Systems*, vol. 33, pp. 11 913–11 924, 2020.

- [17] M. Careil, M. J. Muckley, J. Verbeek, and S. Lathuilière, “Towards image compression with perfect realism at ultra-low bitrates,” in *The Twelfth International Conference on Learning Representations*, 2023.
- [18] L. Theis, T. Salimans, M. D. Hoffman, and F. Mentzer, “Lossy compression with gaussian diffusion,” *arXiv preprint arXiv:2206.08889*, 2022.
- [19] J. Wang, S. Wang, J. Dai, Z. Si, D. Zhou, and K. Niu, “Perceptual learned source-channel coding for high-fidelity image semantic transmission,” in *GLOBECOM 2022-2022 IEEE Global Communications Conference*. IEEE, 2022, pp. 3959–3964.
- [20] P. Isola, J.-Y. Zhu, T. Zhou, and A. A. Efros, “Image-to-image translation with conditional adversarial networks,” in *Proceedings of the IEEE conference on computer vision and pattern recognition*, 2017, pp. 1125–1134.
- [21] E. Erdemir, T.-Y. Tung, P. L. Dragotti, and D. Gündüz, “Generative joint source-channel coding for semantic image transmission,” *IEEE Journal on Selected Areas in Communications*, 2023.
- [22] T. Karras, S. Laine, M. Aittala, J. Hellsten, J. Lehtinen, and T. Aila, “Analyzing and improving the image quality of stylegan,” in *Proceedings of the IEEE/CVF conference on computer vision and pattern recognition*, 2020, pp. 8110–8119.
- [23] S. F. Yilmaz, X. Niu, B. Bai, W. Han, L. Deng, and D. Gunduz, “High perceptual quality wireless image delivery with denoising diffusion models,” *arXiv preprint arXiv:2309.15889*, 2023.
- [24] Y. Wang, J. Yu, and J. Zhang, “Zero-shot image restoration using denoising diffusion null-space model,” in *The Eleventh International Conference on Learning Representations*, 2022.
- [25] R. Rombach, A. Blattmann, D. Lorenz, P. Esser, and B. Ommer, “High-resolution image synthesis with latent diffusion models,” in *Proceedings of the IEEE/CVF conference on computer vision and pattern recognition*, 2022, pp. 10684–10695.
- [26] X. Lin, J. He, Z. Chen, Z. Lyu, B. Fei, B. Dai, W. Ouyang, Y. Qiao, and C. Dong, “Diffbir: Towards blind image restoration with generative diffusion prior,” *arXiv preprint arXiv:2308.15070*, 2023.
- [27] J. Ho, A. Jain, and P. Abbeel, “Denoising diffusion probabilistic models,” *Advances in neural information processing systems*, vol. 33, pp. 6840–6851, 2020.
- [28] J. Hu, L. Shen, and G. Sun, “Squeeze-and-excitation networks,” in *Proceedings of the IEEE conference on computer vision and pattern recognition*, 2018, pp. 7132–7141.
- [29] J. Li, D. Li, S. Savarese, and S. Hoi, “Blip-2: Bootstrapping language-image pre-training with frozen image encoders and large language models,” in *International conference on machine learning*. PMLR, 2023, pp. 19730–19742.
- [30] M. Heusel, H. Ramsauer, T. Unterthiner, B. Nessler, and S. Hochreiter, “Gans trained by a two time-scale update rule converge to a local nash equilibrium,” *Advances in neural information processing systems*, vol. 30, 2017.